Role of carbon dioxide in the ethylbenzene dehydrogenation coupled with reverse water–gas shift

Ailing Sun, Zhangfeng Qin, Shuwei Chen, Jianguo Wang*

State Key Laboratory of Coal Conversion, Institute of Coal Chemistry, Chinese Academy of Sciences, P.O. Box 165, Taiyuan, Shanxi 030001, PR China

Abstract

The dehydrogenation of ethylbenzene (EB) to styrene (ST) in the presence of carbon dioxide instead of steam is believed to be an energy-saving and environmentally friendly process. However, the reaction mechanism for this coupling system still remains unclear. Therefore, the role of carbon dioxide was investigated by means of catalytic reactions and temperature-programmed desorption (TPD) of carbon dioxide over a series of Fe and V supported catalysts as well as thermodynamic analysis. The results showed that the ethylbenzene conversion is associated with the conversion of carbon dioxide, and that there exists a synergistic effect between the ethylbenzene dehydrogenation and the reverse water–gas shift. However, the difference in the behaviour of the catalysts between the single reverse water–gas shift and the coupled ethylbenzene dehydrogenation may suggest that the catalysts are different in the reaction mechanisms for the coupled ethylbenzene dehydrogenation. Carbon dioxide can be activated through either basic sites or redox sites on the catalyst. Based on these results, the role of carbon dioxide and reaction mechanisms are proposed.
© 2003 Elsevier B.V. All rights reserved.

Keywords: Reaction coupling; Ethylbenzene dehydrogenation; Water–gas shift; Carbon dioxide; Styrene

1. Introduction

Styrene (ST) is commercially produced by the dehydrogenation of ethylbenzene (EB) on the promoted iron oxide catalysts at 600–700 °C, just below the temperature where thermal cracking becomes significant. Due to its highly endothermic and volume-increasing character, a large amount of superheated steam is used to supply heat, lower the partial pressure of the reactant, and avoid the formation of carbonaceous deposits. However, much of the latent heat of steam is lost in the gas–liquid separator without recovery [1].

The dehydrogenation of EB to ST in the presence of CO_2 instead of steam is believed to be an energy-saving and environmentally friendly process. The equilibrium conversion can be improved through the reaction coupling of EB dehydrogenation with the reverse water–gas shift (RWGS) [2], and it is estimated that the energy required for producing per ton ST in the coupling process is $(1.5–1.9) \times 10^8$ cal,

considerably low compared with 1.5×10^9 cal in the current commercial process [3,4]. Various catalysts have been tested on the EB dehydrogenation in the presence of CO_2 [1,3–16]. Inorganic oxides (Al_2O_3, MgO, ZnO, WO_3, SiO_2 and ZrO_2), various zeolites, as well as a wide range of carbonaceous materials such as active carbon (AC) were used as the supports. Different transition metal oxides (Fe, V, Cr, Cu, Zr, Ce, La, Na, Ni and Co) were adopted as the active components, and the alkaline metals (Li, Na and K), alkali earth metals (Ca and Mg) and other elements (Sb and Cr) were introduced as the promoters. The results proved that the reaction behaviour could be improved greatly by the coupling of EB dehydrogenation with the RWGS.

Several investigations were also conducted to reveal the mechanism of reaction coupling. Sato et al. [5] found that EB was activated by the acidic sites over γ-Al_2O_3 supported catalysts while CO_2 was activated by basic sites; CO_2 conversion was then correlated with the amounts of strong basic sites. Park et al. [7] found that ZrO_2 was active for EB dehydrogenation, especially in the presence of CO_2; the differences in catalytic activity could be ascribed to the differences in the surface area and CO_2 affinity that was associated with the surface basicity of the catalysts.

* Corresponding author. Tel.: +86-351-4046092;
fax: +86-351-4041153.
E-mail address: iccjgw@sxicc.ac.cn (J. Wang).

As for the possible reaction pathway, Mimura and co-workers [3–5] proposed one-step and two-step pathways. The EB dehydrogenation in the presence of CO_2 was considered to proceed both via the one-step and via the two-step pathway; over basic Na_2O/Al_2O_3 catalyst, the one-step pathway was the main route, while over Fe_2O_3/Al_2O_3 catalyst, 45% of ST was produced via the one-step pathway and 55% via the two-step pathway.

As for the reaction mechanism, it was generally accepted that the catalysts behave in accordance with the redox cycle. Sugino et al. [10] and we [14] showed that over Fe/AC catalyst, iron oxides in a high valence state of Fe such as $LiFe_5O_8$ or Fe_3O_4 seemed to be the active phases for the coupled reaction and CO_2 played an important role in keeping the iron species at high valence. Sakurai et al. [11,12] claimed that the active species over V/AC, Cr/AC and Ce/AC catalysts were V_2O_5, Cr_2O_3, and CeO_2, respectively; the valence of these species changed following the redox cycle. Chang et al. [15] also suggested that CO_2 could be activated by the oxygen deficiency in the catalyst and dissociated into CO and surface oxygen. The surface oxygen may play an important role in the dehydrogenation and the coke removal.

Although some general conclusions have been made on the EB dehydrogenation in the presence of CO_2, the detailed reaction mechanism and the role of CO_2 in the coupling system still remain unclear. For example how the conversions of EB and CO_2 were related to the different pathways? Coupling effects were observed over various catalysts, but the RWGS behaved differently over these catalysts; what is the difference between the single RWGS (only with CO_2 and H_2 as reactants) and the RWGS in the coupled EB dehydrogenation in the presence of CO_2?

In the present paper, the performances of various Fe and V supported catalysts on the EB dehydrogenation in the presence/absence of CO_2 were examined, and the role of CO_2 was investigated by means of catalytic reactions and temperature-programmed desorption (TPD) of CO_2 as well as thermodynamic analysis. The results showed that the EB conversion is associated with the conversion of CO_2, and that there exists a synergistic effect between the EB dehydrogenation and the RWGS. However, the difference in the behaviour of the catalysts between the single RWGS and the coupled EB dehydrogenation may suggest that the catalysts are different in the reaction mechanisms for the coupled EB dehydrogenation. CO_2 can be activated through either basic sites or redox sites on the catalyst. Based on these results, the role of CO_2 and reaction mechanisms are proposed.

2. Experimental

2.1. Catalyst preparation

All the catalysts in this study were prepared by impregnation or co-impregnation method. γ-Al_2O_3 (obtained from Institute of Coal Chemistry, Chinese Academy of Science)

with a BET area of $275\,m^2/g$, a pore volume of $0.70\,cm^3/g$ and an average pore aperture of 10 nm was used as the catalyst supports. The supports were first crashed and sieved to 20–40 mesh, and then activated at $500\,°C$ for 2 h before use. The active components Fe and V were introduced by impregnation of the supports with aqueous solutions of iron nitrate and NH_4VO_3 dissolved in an aqueous solution of oxalic acid, respectively. Alkali metal (Li), alkaline earth metal (Ca) and transition metal (Mn, Cr) promoted catalysts were prepared by co-impregnation with a solution containing both the active components and the nitrates of the promoters. The impregnation treatment lasted for 18 h, and then the catalysts were dried at $120\,°C$ in air for 4 h. Then the catalyst V/Al_2O_3 was calcined at $550\,°C$ in air for 4 h, while Fe/Al_2O_3 at $650\,°C$ for 5 h. The combined catalyst $Fe-V/Al_2O_3$ was prepared by the multiple-step impregnation: the Al_2O_3 support was first impregnated with iron nitrate solution followed by calcination at $650\,°C$ in air for 5 h; and then the Fe/Al_2O_3 obtained was impregnated with NH_4VO_3 dissolved in an aqueous solution of oxalic acid, followed by calcination at $550\,°C$ in air for 4 h. Impregnation in this order is due to the fact that the calcination temperature for Fe/Al_2O_3 was higher than that for V/Al_2O_3, and such a consideration was also helpful to avoid V-loss during the catalyst preparation.

In order to compare with the reaction results of carbonaceous supported catalysts, some catalysts with AC as support were also prepared according to the methods as described in our previous report [14].

2.2. Reaction and analytical procedures

The catalytic reaction was performed in a stainless steel tube reactor with ϕ 6.0 mm i.d., and about 200 mg catalyst was used per run. Before the reaction, the catalyst was first activated under a nitrogen flow from the room temperature to reaction temperature, and then the nitrogen flow was switched to CO_2 when the reaction was intended to be operated in the presence of CO_2. The catalyst was maintained at this temperature for 10 min before introducing EB (20.4 mmol-EB/(g-cat h)) by a micro feeder pump. The molar ratio of CO_2 to EB was fixed at 11 and the W/F was controlled at 4.07 g-cat h/mol. The reaction was operated at $550\,°C$ at atmospheric pressure. The effluents, including ST, benzene, toluene, and unreacted EB were condensed in a trap with an ice water bath.

As for the single RWGS, the catalyst evaluation was carried out in the mixture of CO_2 and H_2 in the same reactor as for the EB dehydrogenation. The molar ratio of CO_2 to H_2 was fixed at 11 and the W/F was controlled at about 2.04 g-cat h/mol.

The liquid products were analyzed with an FID gas chromatograph (Shimadzu GC-7A) equipped with a 3 mm × 3 m stainless-steel column packed with OV-101. The gaseous products (H_2, N_2, CO, CO_2, CH_4, and C_2H_6) were analyzed by a TCD gas chromatograph (Shimadzu GC-9A) equipped with a 3 mm × 3 m stainless-steel column packed with carbon

molecular sieve. The conversion of CO_2 was simply defined as $x_{CO}/(x_{CO} + x_{CO_2})$, where x_{CO} and x_{CO_2} are the molar fractions of CO and CO_2, respectively in the effluent gas.

2.3. CO_2-TPD

The surface basicity of the catalysts was determined by the CO_2-TPD in a micro reactor followed by a mass spectroscopy (Omni Star 200), and about 200 mg catalyst was used per run. The catalyst sample was first heated up to 550 °C under nitrogen atmosphere and kept at this temperature for 1 h, and then cooled down to 100 °C. The pulse of CO_2 was then introduced until the adsorption of CO_2 on the catalyst was saturated. After that, TPD was performed under nitrogen at 100–800 °C with a heating rate of 12 °C/min and the exhaust gases were detected by the mass spectrometry.

3. Results and discussion

3.1. Two pathways viewed on the basis of thermodynamic analysis

As proposed by Mimura and Saito [3], EB dehydrogenation in the presence of CO_2 may proceed in two pathways, namely one-step and two-step pathways. For the one-step pathway, EB is oxidized to ST with CO_2 through the direct interaction of CO_2 and EB:

$$C_6H_5–C_2H_5 + CO_2 \rightarrow C_6H_5–C_2H_3 + CO + H_2O \qquad (1)$$
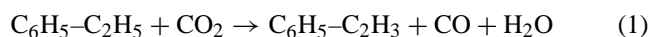
while for the two-step pathway, EB is first dehydrogenated to ST with H_2 formed simultaneously, and then CO_2 reacts with H_2 via the RWGS:

$$C_6H_5–C_2H_5 \rightarrow C_6H_5–C_2H_3 + H_2 \qquad (2\text{-}1)$$

$$H_2 + CO_2 \rightarrow CO + H_2O \qquad (2\text{-}2)$$
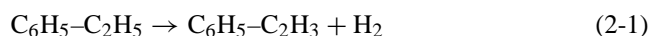
Since H_2 produced in the EB dehydrogenation is eliminated simultaneously by RWGS, the EB conversion can be then improved through the shift of dehydrogenation equilibrium.

To examine the contribution of each pathway, the equilibrium conversions of EB and CO_2 for the coupled EB dehydrogenation in the presence of CO_2 in both one-step and two-step pathways were evaluated according to the method described elsewhere [2]. As shown in Fig. 1, the equilibrium conversions of EB with the coupling via either pathway are higher than those of EB dehydrogenation in the presence of N_2 that has only dilution effect. EB conversion of the coupled dehydrogenation via the two-step pathway is a little higher than that via the one-step pathway at 350–600 °C; in contrast, the CO_2 conversion via the two-step pathway is much lower at a temperature higher than 450 °C. Moreover, there will be no H_2 in the effluent gas when the reaction follows solely the one-step pathway.
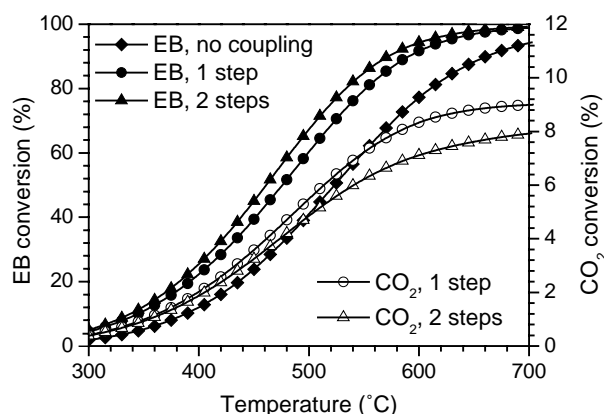

Fig. 1. Equilibrium conversion of EB and CO_2 under 0.1 MPa: for EB dehydrogenation in the presence of N_2 (no coupling), initial N_2:EB = 11; for the coupled EB dehydrogenation in the presence of CO_2 (in one step or two steps), initial CO_2:EB = 11.

3.2. Synergistic effect in the reaction coupling

The catalytic behaviour of Fe and V supported on γ-Al_2O_3 for the EB dehydrogenation in the presence of CO_2 or N_2 was investigated at 550 °C. A comparison of the results with both reaction coupling (in the presence of CO_2) and non-coupling (in the presence of N_2) were listed in Table 1. It can be seen that the EB conversion was greatly improved through the reaction coupling. Furthermore, the Fe/Al_2O_3 and V/Al_2O_3 catalysts, showing almost the same activity in the non-coupling system, performed differently in the coupling system; V/Al_2O_3 showed much higher activity than Fe/Al_2O_3 in the coupled EB dehydrogenation. However, all the results indicated that for the coupled EB dehydrogenation in the presence of CO_2, the catalyst which gave a good ST yield also showed a high CO_2 conversion.

Table 1
EB dehydrogenation in the presence of CO_2 or N_2 over Fe, V supported on γ-Al_2O_3

Active components[a]	Atmosphere	EB conversion (%)	ST yield (%)	CO_2 conversion (%)
Fe(3)	CO_2	35.0	33.7	1.7
Fe(3)	N_2	34.2	32.9	–
Fe(3)Ca(0.3)	CO_2	39.0	37.9	2.7
Fe(3)Mn(0.3)	CO_2	37.8	37.0	2.6
Fe(3)Cr(0.3)	CO_2	42.9	42.0	3.5
Fe(2)V(0.58)	CO_2	48.6	48.0	3.0
V(0.57)	CO_2	45.5	44.5	4.3
V(0.57)	N_2	37.4	36.7	–
V(0.57)Mn(0.3)	CO_2	41.9	41.3	4.3
V(0.57)Cr(0.3)	CO_2	50.3	49.2	5.5
V(0.57)Cr(0.3)	N_2	43.0	41.7	–

[a] The element labels and numerals in parentheses indicate the active components and their loadings in mmol/(g-support); reactions were carried out under 550 °C, atmospheric pressure, W/F = 4.07 g-cat h/mol, CO_2/EB = 11 (in the presence of CO_2) and N_2/EB = 11 (in the presence of N_2); data was acquired after reaction lasted for 3 h.
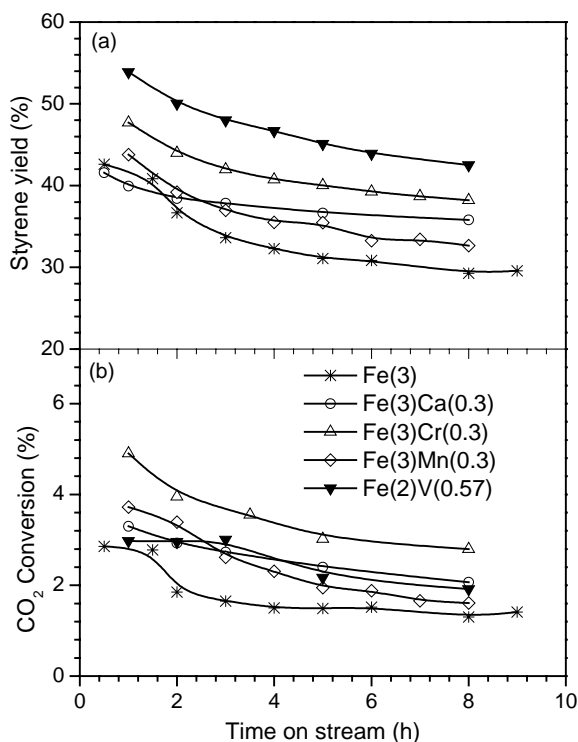
Fig. 2. ST yield (a) and CO_2 conversion (b) with the time on stream for the coupled EB dehydrogenation in the presence of CO_2 over Fe/Al_2O_3 modified by various promoters: the element labels and numerals in parentheses indicate the active components and their loadings in mmol/(g-support); the reaction was carried out at 550 °C, 0.1 MPa, $CO_2/EB = 11$, and W/F = 4.07 g-cat h/mol.
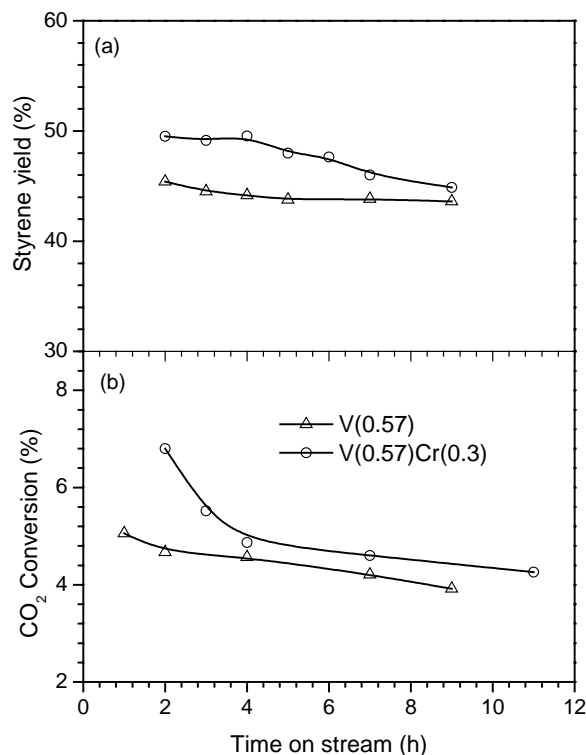

Fig. 3. ST yield (a) and CO_2 conversion (b) with the time on stream for the coupled EB dehydrogenation in the presence of CO_2 over V/Al_2O_3: the specifications are the same as shown in Fig. 2.

As shown in Fig. 2, over Fe/Al_2O_3 catalysts modified by various promoters the conversion of CO_2 showed primarily the same tendency as the conversion of EB with the time on stream; the higher the CO_2 conversion, the higher the EB conversion. The same phenomenon was also observed over V/Al_2O_3 (Fig. 3) and AC supported catalysts [14]. Namely, there exists a synergistic effect between the EB dehydrogenation and the RWGS in the coupling system; the EB conversion is associated with the conversion of CO_2 for the coupled EB dehydrogenation in the presence of CO_2.

3.3. Different behaviour of CO_2 in the coupled EB dehydrogenation and in the single RWGS

To investigate the reaction mechanism and the role of CO_2, the CO_2 conversions in the single RWGS over several catalysts were also examined in comparison with that in the coupled EB dehydrogenation. As shown in Fig. 4, for the single RWGS, the order of CO_2 conversion over different catalysts was: $FeCr/Al_2O_3 > Fe/Al_2O_3 > FeV/Al_2O_3 > VCr/Al_2O_3 > V/Al_2O_3$, while in the coupled EB dehydrogenation, the order of CO_2 conversion became: $VCr/Al_2O_3 > V/Al_2O_3 > FeCr/Al_2O_3 > FeV/Al_2O_3 > Fe/Al_2O_3$. For the single RWGS, Fe supported on γ-Al_2O_3, especially promoted by Cr, was an effective catalyst; while

V supported on γ-Al_2O_3 behaved badly. In contrast, for the coupled EB dehydrogenation, V supported on γ-Al_2O_3 showed high CO_2 conversion, which thereon gave also good activity for the EB dehydrogenation to ST, as shown in Table 1 and Figs. 2 and 3. Such a phenomenon was also observed over AC supported Fe or V catalysts, as shown in Fig. 5. It should be noted that in the coupled EB dehydrogenation, H_2 was produced gradually and a complete conversion of EB would never occur; thus the amount of hydrogen in the coupling system was relatively deficient. In addition, the contact time for the single RWGS was only half of that for the coupled EB dehydrogenation in this work. Therefore, a comparison of the absolute values of the CO_2 conversions between the single RWGS and the coupled EB dehydrogenation is impossible. However, it was clearly shown that over V/Al_2O_3 the CO_2 conversion was very low in the single RWGS but high in the coupled EB dehydrogenation. Over Fe/Al_2O_3, the CO_2 conversions in both the single RWGS and the coupled EB dehydrogenation were significantly high.

The different behaviour of CO_2 conversions over Fe/Al_2O_3 and V/Al_2O_3 indicated that the reaction mechanisms for the coupled EB dehydrogenation over different catalysts were quite different, which could result from the different manners of hydrogen species formation and CO_2 activation. As shown in Fig. 6, two kinds of hydrogen species formed from the EB dehydrogenation in the
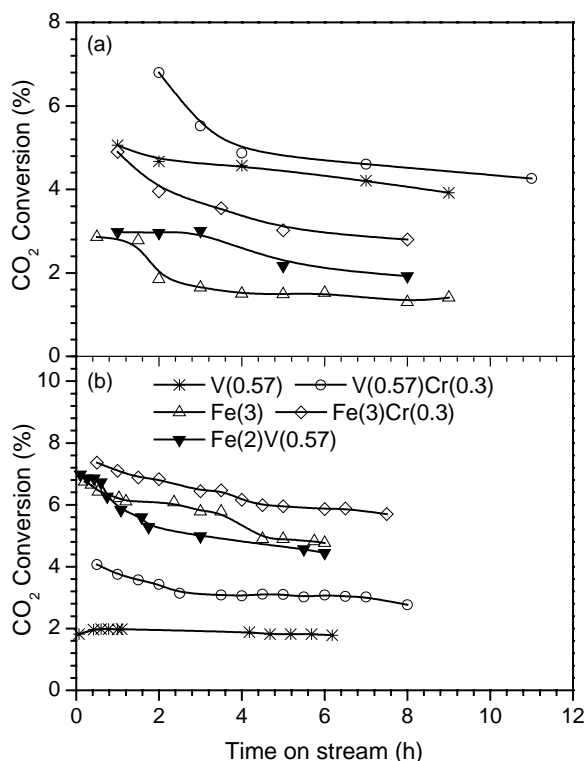
Fig. 4. Comparison of CO_2 conversions in the (a) coupled EB dehydrogenation (reaction conditions are the same as shown in Fig. 2) and (b) single RWGS (the reaction was carried out under 550 °C, 0.1 MPa, $CO_2/H_2 = 11$, and W/F = 2.04 g-cat h/mol) over the catalysts Fe, V supported on γ-Al_2O_3.

Fig. 5. Comparison of CO_2 conversions in the coupled EB dehydrogenation (a) and in the single RWGS (b) over the catalysts Fe and V supported on AC, the specifications are the same as shown in Fig. 4.

presence of CO_2: active hydrogen species (atomic) and molecular hydrogen. CO_2 could either contact directly with the active hydrogen species or react with the molecular hydrogen, which corresponded to the one-step and two-step pathways, respectively.

If the coupled EB dehydrogenation followed completely the one-step pathway, there would be no H_2 in the effluent gas. However, there existed a certain amount of H_2 in the effluent gas for all the catalytic tests, which suggested that both the pathways coexist in the coupled EB dehydrogenation. Moreover, the difference in the behaviour of CO_2 over different catalysts indicated that the catalysts are different in the contribution of each pathway. Fe supported catalysts showed good activity for the single RWGS, which may indicate that the two-step pathway played an important role in the coupled EB dehydrogenation. Over the Fe/Al_2O_3, the CO_2 conversion of 1.7% accounted for about 55% of ST yield; namely, the two-step pathway could contribute as high as 55% of ST produced, which agreed with the observation of Mimura and Saito [3]. On the other hand, V supported catalyst behaved badly in the single RWGS, but showed good activity for the coupled EB dehydrogenation; these may suggest that the one-step pathway played a dominating role in the coupled EB dehydrogenation over the V supported catalyst.
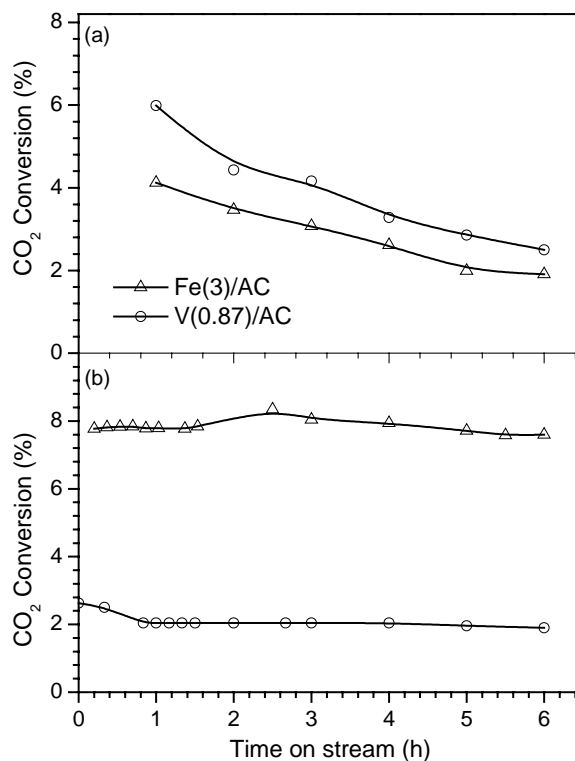
3.4. Activation of CO_2

The differences in CO_2 conversions over different catalysts may also suggest the variation of the manners for the CO_2 activation. In order to characterize the surface basic sites, the CO_2-TPD over Fe and V supported on γ-Al_2O_3 was conducted. As shown in Fig. 7, the amount of basic sites over Fe/Al_2O_3 was apparently larger than that of V/Al_2O_3. Moreover, weak and strong basic sites coexisted over Fe/Al_2O_3, while the strong basic sites over V/Al_2O_3 were detected only after the Cr promoter was added. The strong basic sites may be responsible for the activation of CO_2 at reaction temperature. The promoter Cr could enhance the amounts of strong basic sites (the ridge between 350 and 550 °C in the CO_2-TPD spectra), and thereon improve the activity for the RWGS and coupled EB dehydrogenation in the presence of CO_2.

As for the V/Al_2O_3 with few strong basic sites, CO_2 could be activated primarily through the redox sites on the
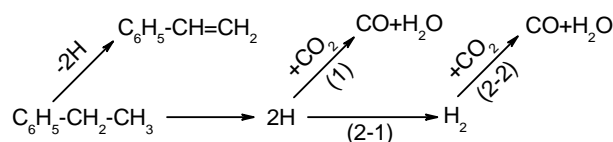
Fig. 6. Role of CO_2 in the coupled EB dehydrogenation in the presence of CO_2.
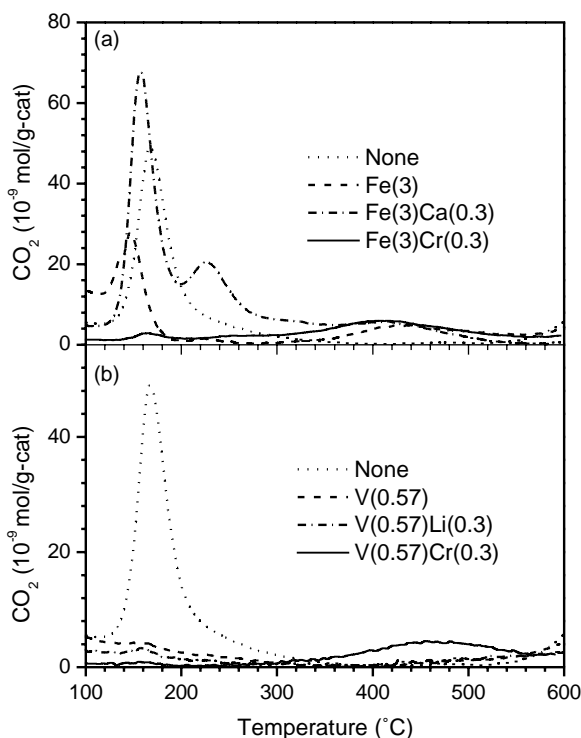
Fig. 7. CO_2-TPD characterization of catalysts Fe (a) and V (b) supported on γ-Al_2O_3: none, pure γ-Al_2O_3 support; the element labels and numerals in parentheses indicate the active components and their loadings in mmol/(g-support).
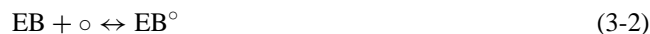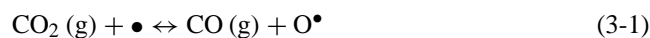
catalysts, since the valence of vanadium is easily changeable. Over the V/Al_2O_3, there existed small amount of V^{4+}, and the deficiencies of oxygen in vanadium oxide could also change the V^{5+} around them into V^{4+}. These two types of V species act as the oxygen carrier in the form of a redox pair [17]. Sakurai et al. [11,12] and Vislovskiy et al. [16] studied the performance of V/AC, V/MgO and V/Al_2O_3 catalysts in the coupled EB dehydrogenation and also proposed that the reaction proceeded according to the redox mechanism. Sugino et al. [10] and we [14] also showed that there existed redox cycles over the Fe/AC catalyst and that CO_2 played an important role in keeping the iron species at high valence.

Therefore, CO_2 can be activated through either the basic sites or the redox sites on the catalysts. Over the Fe supported catalyst with Cr as promoter, the strong basic sites may play an important role, while over V/Al_2O_3 the redox cycle is crucial for the CO_2 activation.
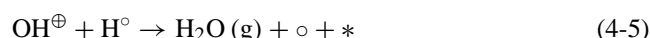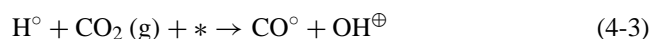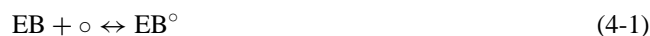
3.5. Possible reaction mechanisms

Based on the above discussions and considering that EB was activated by the oxidative/acidic sites over γ-Al_2O_3 supported catalysts [5] and that the catalysts behaved according to the redox cycle during the reaction process in the presence of CO_2 [10,14], three possible mechanisms for the coupled EB dehydrogenation in the presence of CO_2 are proposed.
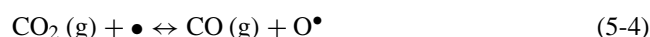
Mechanism-1 ($\circ$, oxidative site; $\bullet$ reductive site):

$$CO_2\,(g) + \bullet \leftrightarrow CO\,(g) + O^{\bullet} \qquad (3\text{-}1)$$

$$EB + \circ \leftrightarrow EB^{\circ} \qquad (3\text{-}2)$$

$$O^{\bullet} + EB^{\circ} \rightarrow ST^{\bullet} + H_2O^{\circ} \qquad (3\text{-}3)$$

$$ST^{\bullet} \rightarrow ST + \bullet \qquad (3\text{-}4)$$

$$H_2O^{\circ} \rightarrow H_2O\,(g) + \circ \qquad (3\text{-}5)$$

Mechanism-2 ($\oplus$/$\circ$, acid/oxidative site; $*$/$\bullet$, basic/reductive site):

$$EB + \circ \leftrightarrow EB^{\circ} \qquad (4\text{-}1)$$

$$EB^{\circ} + \circ + \bullet \rightarrow ST^{\bullet} + 2H^{\circ} \qquad (4\text{-}2)$$

$$H^{\circ} + CO_2\,(g) + * \rightarrow CO^{\circ} + OH^{\oplus} \qquad (4\text{-}3)$$

$$CO^{\circ} \leftrightarrow CO\,(g) + \circ \qquad (4\text{-}4)$$

$$OH^{\oplus} + H^{\circ} \rightarrow H_2O\,(g) + \circ + * \qquad (4\text{-}5)$$

$$ST^{\bullet} \rightarrow ST + \bullet \qquad (4\text{-}6)$$

Mechanism-3 ($\circ$, oxidative site; $\bullet$, reductive site):

$$EB + \circ \leftrightarrow EB^{\circ} \qquad (5\text{-}1)$$

$$EB^{\circ} + \circ + \bullet \rightarrow ST^{\bullet} + 2H^{\circ} \qquad (5\text{-}2)$$

$$H^{\circ} + H^{\circ} \rightarrow H_2\,(g) + 2\circ \qquad (5\text{-}3)$$

$$CO_2\,(g) + \bullet \leftrightarrow CO\,(g) + O^{\bullet} \qquad (5\text{-}4)$$

$$H_2\,(g) + O^{\bullet} \leftrightarrow H_2O\,(g) + \bullet \qquad (5\text{-}5)$$

$$ST^{\bullet} \rightarrow ST + \bullet \qquad (5\text{-}6)$$

Mechanisms 1 and 2 can be generalized to the one-step pathway, while the mechanism 3 leads to the two-step pathway. In all cases, CO_2 plays an important role in keeping the active sites for EB dehydrogenation at high valence. It is possible that all these mechanisms coexisted, but the proportion of each mechanism would depend on the catalysts used in the coupled EB dehydrogenation. Over a certain catalyst such as V/Al_2O_3, the coupled EB dehydrogenation might proceeds mainly via mechanism 1, while over Fe/Al_2O_3, mechanisms 2 and 3 might play an important role. However, considerable work is still necessary to make clear the mechanism of EB dehydrogenation in the presence of CO_2.

4. Conclusions

The role of CO_2 in the coupled EB dehydrogenation was investigated by means of catalytic reactions and CO_2-TPD over a series of Fe and V supported catalysts as well as thermodynamic analysis. The results showed that the EB conversion is associated with the conversion of CO_2, and that

there exists a synergistic effect between the EB dehydrogenation and the RWGS. The difference in the behaviour of the catalysts between the single RWGS and the coupled EB dehydrogenation may suggest that the catalysts are different in the reaction mechanisms for the coupled EB dehydrogenation. CO_2 can be activated through either basic sites or redox sites on the catalyst. Based on these results, the role of CO_2 and reaction mechanisms are proposed. They are dependent on the catalyst used in the coupled EB dehydrogenation. Over the Fe/Al_2O_3 the two-step pathway played an important role, while over the V/Al_2O_3 the one-step pathway dominated the reaction.

Acknowledgements

References

[1] J. Matsui, T. Sodesawa, F. Nozaki, Appl. Catal. A 67 (1991) 179.

[2] Z. Qin, J. Liu, A. Sun, J. Wang, Ind. Eng. Chem. Res. 42 (2003) 1329.

[3] N. Mimura, M. Saito, Catal. Lett. 58 (1999) 59.

[4] N. Mimura, M. Saito, Catal. Today 55 (2000) 173.

[5] N. Mimura, I. Takahara, M. Saito, T. Hattori, K. Ohkuma, M. Ando, Catal. Today 45 (1998) 61.

[6] S. Sato, M. Ohhara, T. Sodesawa, F. Nozaki, Appl. Catal. A 37 (1988) 207.

[7] J. Park, J. Noh, J. Chang, S. Park, Catal. Lett. 65 (2000) 75.

[8] T. Badstube, H. Papp, P. Kustrowski, R. Dziembaj, Catal. Lett. 55 (1998) 169.

[9] T. Badstube, H. Papp, R. Dziembaj, P. Kustrowski, Appl. Catal. A 204 (2000) 153.

[10] M. Sugino, H. Shimada, T. Turuda, H. Miura, N. Ikenaga, T. Suzuki, Appl. Catal. A 121 (1995) 125.

[11] Y. Sakurai, T. Suzaki, N. Ikenaga, T. Suzuki, Appl. Catal. A 192 (2000) 281.

[12] N. Ikenaga, T. Tsuruda, K. Senma, T. Yamaguchi, Y. Sakurai, T. Suzuki, Ind. Eng. Chem. Res. 39 (2000) 1228.

[13] Y. Sakurai, T. Suzaki, K. Nakagawa, N. Ikenaga, H. Aota, T. Suzuki, J. Catal. 209 (2002) 16.

[14] A. Sun, Z. Qin, J. Wang, Appl. Catal. A 234 (2002) 179.

[15] J. Chang, S. Park, M. Park, Chem. Lett. 26 (1997) 1123.

[16] V. Vislovskiy, J. Chang, M. Park, S. Park, Catal. Commun. 3 (2002) 227.

[17] C.N. Satterfield, Heterogeneous Catalysis in Practice, McGraw-Hill, New York, 1999.